Oxygen displacements and search for magnetic order in $Sr_3Ru_2O_7$

Q. Huang
NIST Center for Neutron Research, National Institute of Standards and Technology, Gaithersburg, Maryland 20899 and Department of Materials and Nuclear Engineering, University of Maryland, College Park, Maryland 20742

J. W. Lynn and R. W. Erwin
NIST Center for Neutron Research, National Institute of Standards and Technology, Gaithersburg, Maryland 20899

J. Jarupatrakorn and R. J. Cava
Department of Chemistry and Materials Institute, Princeton University, Princeton, New Jersey 08540
(Received 19 March 1998)

The crystal structure of the layered $Sr_3Ru_2O_7$ system has been analyzed by neutron powder diffraction methods. The structure is formed by stacking two blocks of distorted $SrRuO_3$ perovskite along the c axis, interleaved with SrO layers. The neighboring corner-sharing octahedra in each double perovskite block are rotated with respect to each other about the vertical axis so that the Ru-O-Ru angle in the RuO_2 planes is about 165° rather than 180°. These rotations are correlated within each double perovskite block, but they are not correlated along the c axis, resulting in an intrinsic disorder that emphasizes the layered nature of this material. The resulting structure has the symmetry of space group *Pban* and lattice parameters $a=b=5.5016(1)$ Å and $c=20.7194(5)$ Å at 295 K. Data taken to 9 K showed no evidence of any structural phase transitions occurring below room temperature. We also searched for the development of long-range magnetic order to temperatures as low as 1.6 K, but no evidence of either ferromagnetic or antiferromagnetic long-range order was observed, with an upper limit of $0.05\mu_B$ for any possible ordered moment. This result contrasts with a reported ferromagnetic ordering at 104 K with an ordered Ru moment of $1.3\mu_B$, which we believe was due to a phase other than $Sr_3Ru_2O_7$. We also searched for an induced moment, for applied fields up to 7 T, but did not observe any induced ferromagnetic moment within the same experimental limit. [S0163-1829(98)00638-9]

INTRODUCTION

The strontium ruthenates $SrRuO_3$ and Sr_2RuO_4 have been the subject of renewed interest due to their magnetic and electronic properties, and their compatibility with cuprate perovskites when used as metallic conducting electrodes.[1–8] The three-dimensional perovskite $SrRuO_3$ is a metallic high-T_c ferromagnet ($T_c=160$ K) with a full Ru^{4+} moment above T_c and an ordered moment of $1\mu_B$/Ru. The K_2NiF_4-type layered oxide Sr_2RuO_4, in contrast, shows no local-moment magnetism or long-range magnetic ordering, and in fact is a low-T_c superconductor whose properties suggest that it may be an exotic superconductor.[9–11] The compound $Sr_3Ru_2O_7$ has a double layer of RuO_6 octahedra, and therefore may be expected to have properties intermediate between those of $SrRuO_3$ and Sr_2RuO_4. Although known for some time,[12–15] it has been characterized only recently. It was first reported to be an antiferromagnetic metal, with a Curie-Weiss susceptibility corresponding to a full Ru^{4+} moment and developing antiferromagnetic spin correlations below 15 K.[16] It was later reported to be an itinerant ferromagnet, with a T_c near 104 K and ordered moments of approximately $1.3\mu_B$/Ru, similar to that observed for $SrRuO_3$.[17] Here we report the results of a neutron diffraction powder profile analysis determination of the crystal structure of this phase at ambient temperature and at 9 K. The results show that there is rotation of neighboring RuO_6 octahedra in the RuO_2 planes through their shared oxygen atoms, such that the Ru-O-Ru bond angles in the plane are considerably distorted from the ideal 180°. The rotations are correlated within the double layers but are not correlated along the stacking axis. The low-temperature data show no evidence for long-range three-dimensional ordering of the magnetic moment, either ferromagnetically or antiferromagnetically.

EXPERIMENT

A 3-g powder sample of $Sr_3Ru_2O_7$ was prepared as described elsewhere.[11] It is worth pointing out that the final reaction step consisted of heating the 1-g pellets in oxygen at 1300 °C, and then quenching them on an Al plate. We have found that if this quenching step is not performed, then $Sr_3Ru_2O_7$ partially decomposes into Sr_2RuO_4 and $SrRuO_3$, which can be present as intergrowths in crystalline $Sr_3Ru_2O_7$.[11] We note that even for impurity levels as low as 50 ppm, the presence of $SrRuO_3$ can make a strontium ruthenium oxide sample appear to be ferromagnetic with a T_c as high as 160 K.[8,11]

The neutron powder diffraction intensity data were collected using the BT-1 high-resolution powder diffractometer located at the reactor of the National Institute of Standards and Technology Center for Neutron Research. A Cu(311) monochromator was employed to produce a monochromatic neutron beam of wavelength of 1.5396(1) Å. Collimators with horizontal divergences of 15′, 20′, and 7′ full width at half maximum were used before and after the monochromator, and after the sample, respectively. The intensities were measured in steps of 0.05° in the 2θ range 3°–168°.

TABLE I. Refinement results for $Sr_3Ru_2O_7$ obtained from models with $I4/mmm$ (No. 139) symmetry. Constrained $B_{Sr(1)}=B_{Sr(2)}$. $B=8\pi^2\langle u^2\rangle$, and $B_{ij}=8\pi^2\langle u_{ij}^2\rangle$, where u is the mean-square displacement and i,j is x, y, or z.

				295 K		
Atom	Site and position		Parameter	Model I	Model II	Model III
			a (Å)	3.8903(1)	3.890 10(9)	3.890 11(9)
			c (Å)	20.7194(8)	20.7186(6)	20.7185(6)
			V (Å^3)	313.58(3)	313.53(2)	313.53(2)
Sr(1)	2b	$(\frac{1}{2},\frac{1}{2},0)$	B (Å^2)	0.67(4)	0.71(2)	0.62(2)
Sr(2)	4e	$(\frac{1}{2},\frac{1}{2},z)$	z	0.1864(1)	0.186 45(7)	0.186 40(8)
			B (Å^2)	0.85(4)	0.88(2)	0.79(3)
Ru	4e	(0,0,z)	z	0.0976(1)	0.0977(1)	0.097 69(9)
			B (Å^2)	0.33(4)	0.60(3)	0.52(3)
O(1)	2a	(0,0,0)	B (Å^2)	1.35(4)	1.48(3)	1.34(3)
O(2)	4e	(0,0,z)	z	0.1942(1)	0.1950(1)	0.1950(1)
			B (Å^2)	0.84(4)	0.97(3)	0.83(3)
O(3)	8g	$(\frac{1}{2},0,z)$	z	0.0970(2)	0.097 00(9)	
			B (Å^2)	2.61(5)		
			B_{11} (Å^2)		0.12(6)	
			B_{22} (Å^2)		7.7(2)	
			B_{33} (Å^2)		0.88(8)	
O(3′)	16n	$(\frac{1}{2},y,z)$	y			0.0636(4)
			z			0.0962(1)
			B (Å^2)			0.60(3)
			n			
			R_p (%)	8.50	6.33	6.20
			R_{wp} (%)	11.18	8.15	7.95
			χ^2	4.468	2.374	2.262

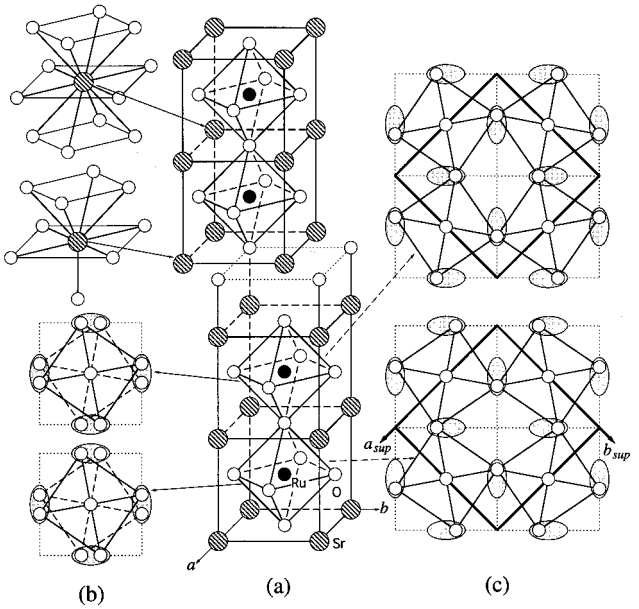

FIG. 1. Arrangements of RuO_6 octahedra within the block of the bilayers. (a) Oxygen atoms on the RuO_2 planes located at the ideal positions, with symmetry $I4/mmm$, Table I, model I; (b) oxygen sites on the RuO_2 planes split into two positions, with 50% occupancy for each. The crystal structure retains $I4/mmm$ symmetry on the average (Table I, model III); (c) the rotations of RuO_6 octahedra within the block of the bilayers are correlated, and the superlattice parameters are related to the tetragonal body-centered lattice by the transformation matrix (1,−1, 0/1, 1, 0/0, 0, 1).

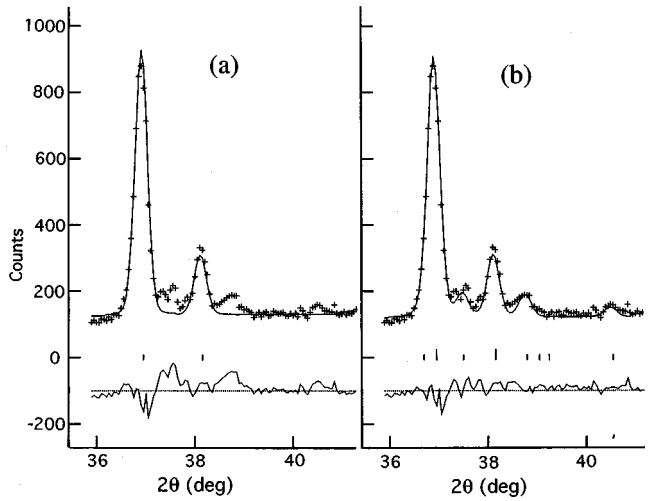

FIG. 2. Portions of the observed (cross) and calculated (solid curve) intensity profiles using different structural models for $Sr_3Ru_2O_7$ at 295 K. (a) Showing some unindexed extra peaks when calculated with model III; (b) calculated with the superlattice model (the shorter vertical lines indicate the possible angular positions for superlattice Bragg reflections).

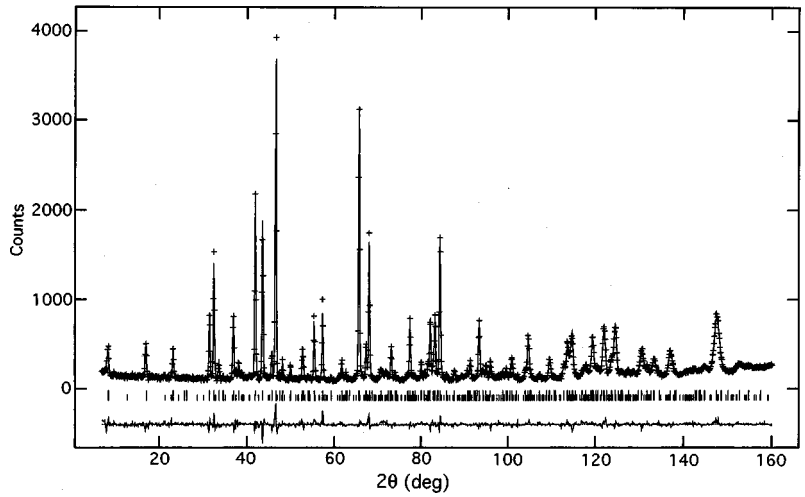

FIG. 3. Plot of observed (crosses) and calculated (solid curve) intensity profiles for $Sr_3Ru_2O_7$ at 295 K. The vertical lines indicate the angular positions for Bragg reflections and the shorter lines show the positions of the superlattice lines. The lower part of the figure shows the difference plot, $I(\text{obs})-I(\text{calc})$.

Data were collected at 295 and 9 K to elucidate possible structural transitions. The structure refinements were carried out using the program GSAS.[18] The neutron scattering amplitudes used in the calculations are 0.702, 0.721, and 0.581 ($\times 10^{-12}$ cm) for Sr, Ru, and O, respectively.

In order to detect possible long-range magnetic order at low temperature, diffraction data were collected from 1.4 to 250 K using the BT-9 triple-axis spectrometer with a pyrolytic graphite PG(002) monochromator. A PG filter was also employed, at a neutron wavelength of 2.359 Å. Relatively coarse collimation was also employed, with the combined effect that this setup provided much higher intensity than BT-1, but with a corresponding reduction in resolution. Measurements were also performed in a 7-T vertical field superconducting magnet in the temperature range from 4.5 to 25 K, in order to search for an induced magnetic moment.

STRUCTURE REFINEMENT

The structure of $Sr_3Ru_2O_7$ determined by single-crystal x-ray techniques, having symmetry $I4/mmm$ and lattice parameters $a=3.890$ Å and $c=20.719$ Å,[13] was adopted as the initial model for our structural refinements. Preliminary calculations showed that the agreement factors for this model (Table I, model I) were much higher than one would expect for a well-refined structure. In addition, the O(3) oxygen atom located on the RuO_2 layers was found to have an unusually large temperature factor (2.61 Å^2), as was also reported in the original x ray.[13] Refinements with an anisotropic temperature factor for O(3) gave a particularly large B_{22} value of 7.7(2) Å^2 and resulted in a significant improvement in the agreement factor R, as shown in Table I, model II. Since this anomalous result may be due to static disorder, a subsequent refinement was carried out with the O(3) site, originally at $\frac{1}{2}$, 0, z, split over the positions $\frac{1}{2}$, y, z (site 16n) of space group $I4/mmm$, with an assigned occupancy of 0.5. As shown in Table I, model III, the refinement yielded a better agreement factor R, and O(3) shifted ~0.24 Å away from the mirror with a much more reasonable thermal parameter of 0.60(3) Å^2.

The structure of $Sr_3Ru_2O_7$, corresponding to model III shown in Fig. 1, is formed by blocks of two $SrRuO_3$ perovskite units interleaved with SrO layers along the c axis. The O(3) displacement (~0.24 Å) indicates that there is a rotation by ~7° of neighboring RuO_6 octahedra in the RuO_2 planes through their corner-shared oxygen atoms, such that the Ru-O-Ru bond angles in the plane are considerably distorted from the ideal 180°. The rotations in each block are not correlated in this model, nor are the blocks coherently arranged along the vertical direction, similar to the structure found for $Sr_3Ir_2O_7$.[20] The calculated intensity profile for this model, however, did not account for a number of weak extra peaks present in the observed diffraction pattern [Fig. 2(a)]. These peaks can be indexed on a superlattice with $a_{\text{sup}}=b_{\text{sup}}=a\sqrt{2}$, and $c_{\text{sup}}=c$, where a and c are the lattice parameters of the tetragonal unit cell. This result indicates that the arrangement of rotations of the RuO_6 octahedra are correlated within the block of the two perovskite units, and may be coherent also along the vertical axis. Models with different arrangements were generated for further refinements. The best result ($R_p=5.65$, $R_{wp}=6.70$, and $\chi^2=1.609$) was obtained with a model in which the rotations of RuO_6 octahedra are correlated within the block of the bilayers [Fig. 1(c)], but are not coherent between blocks stacked along the c axis. The orthorhombic symmetry of space group $Pban$, with superlattice parameters of $a_{\text{sup}}=b_{\text{sup}}=a\sqrt{2}$ and $c_{\text{sup}}=c$, was assumed in the refinements. Since the superstructure is caused by the rotation of RuO_6 octahedra in the opposite sense within the block of bilayers, Sr, Ru, and the O atoms of the SrO layers are constrained to have the same arrangement as those found in model III, and the amplitudes of the displacements of the O atoms in the RuO_2 planes were constrained to be equal. With this model the superlattice peaks were fit very well, as shown in Fig. 2(b). No extra peaks with intensities higher than 2% of the strongest one were found in the final calculation. The same model was used for the refinements of structures at 25 and 9 K. No additional structural distortions or magnetic ordering were found for this sample in these experiments. Figure 3 shows the observed

TABLE II. Structural parameters of $Sr_3Ru_2O_7$ obtained from the refinement of the superlattice model IV with *Pban* symmetry. Only one site occupied for O(31) and O(32).

Atom	Site	and position	Parameter	295 K	25 K	9 K	Constraint
			a_{sup} (Å)	5.5016(1)	5.4770(1)	5.4769(1)	
			b_{sup} (Å)	5.5016(1)	5.4770(1)	5.4769(1)	$=a_{sup}$
			c_{sup} (Å)	20.7194(5)	20.7978(5)	20.7963(6)	
			V_{sup} (Å^3)	627.12(3)	623.88(4)	623.79(4)	
Sr(11)	2*a*	$(\frac{1}{4},\frac{1}{4},0)$	B (Å^2)	0.61(4)	0.17(5)	0.15(4)	
Sr(12)	2*c*	$(\frac{3}{4},\frac{1}{4},\frac{1}{2})$	B (Å^2)	0.61(4)	0.17(5)	0.15(4)	$=B_{Sr(11)}$
Sr(21)	4*k*	$(\frac{1}{4},\frac{1}{4},z)$	z	0.186 30(7)	0.186 63(8)	0.186 69(8)	
			B (Å^2)	0.64(3)	0.32(4)	0.33(4)	
Sr(22)	4*l*	$(\frac{3}{4},\frac{1}{4},z)$	z	0.313 70(7)	0.313 37(8)	0.313 31(8)	$=\frac{1}{2}-z_{Sr(21)}$
			B (Å^2)	0.64(3)	0.32(4)	0.33(4)	$=B_{Sr(21)}$
Ru(1)	4*l*	$(\frac{3}{4},\frac{1}{4},z)$	z	0.097 74(9)	0.0972(1)	0.0974(1)	
			B (Å^2)	0.39(2)	0.30(3)	0.26(3)	
Ru(2)	4*k*	$(\frac{1}{4},\frac{1}{4},z)$	z	0.402 26(9)	0.4028(1)	0.4026(1)	$=\frac{1}{2}-z_{Ru(1)}$
			B (Å^2)	0.39(2)	0.30(3)	0.26(3)	$=B_{Ru(1)}$
O(11)	2*b*	$(\frac{3}{4},\frac{1}{4},0)$	B (Å^2)	1.16(6)	0.32(6)	0.51(7)	
O(12)	2*d*	$(\frac{1}{4},\frac{1}{4},\frac{1}{2})$	B (Å^2)	1.16(6)	0.32(6)	0.51(7)	$=B_{O(11)}$
O(21)	4*l*	$(\frac{3}{4},\frac{1}{4},z)$	z	0.195 03(9)	0.1954(1)	0.1954(1)	
			B (Å^2)	0.82(4)	0.47(4)	0.40(4)	
O(22)	4*k*	$(\frac{1}{4},\frac{1}{4},z)$	z	0.304 97(9)	0.3046(1)	0.3046(1)	$=\frac{1}{2}-z_{O(21)}$
			B (Å^2)	0.82(4)	0.47(4)	0.40(4)	$=B_{O(21)}$
O(31)	8*m*	(x,y,z)	x	0.4688(2)	0.4647(2)	0.4647(2)	
			y	0.0313(2)	0.0353(2)	0.0353(2)	$=\frac{1}{2}-x_{O(31)}$
			z	0.096 34(9)	0.0968(1)	0.0966(1)	
			B (Å^2)	0.63(3)	0.24(3)	0.20(3)	
			n	1.0	1.0	1.0	
O(32)	8*m*	(x,y,z)	x	0.5312(2)	0.5353(2)	0.5353(2)	$=1-x_{O(31)}$
			y	$-0.0313(2)$	$-0.0353(2)$	$-0.0353(2)$	$=x_{O(31)}-\frac{1}{2}$
			z	0.096 34(9)	0.0968(1)	0.0966(1)	$=z_{O(31)}$
			B (Å^2)	0.63(3)	0.24(3)	0.20(3)	$=B_{O(31)}$
			n	0	0	0	
O(33)	8*m*	(x,y,z)	x	0.5312(2)	0.5353(2)	0.5353(2)	$=1-x_{O(31)}$
			y	0.0313(2)	0.0353(2)	0.0353(2)	$=\frac{1}{2}-x_{O(31)}$
			z	0.403 66(9)	0.4032(1)	0.4034(1)	$=\frac{1}{2}-z_{O(31)}$
			B (Å^2)	0.63(3)	0.24(3)	0.20(3)	$=B_{O(31)}$
			n	0.5	0.5	0.5	
O(34)	8*m*	(x,y,z)	x	0.4688(2)	0.4647(2)	0.4647(2)	$=x_{O(31)}$
			y	$-0.0313(2)$	$-0.0353(2)$	$-0.0353(2)$	$=x_{O(31)}-\frac{1}{2}$
			z	0.403 66(9)	0.4032(1)	0.4034(1)	$=\frac{1}{2}-z_{O(31)}$
			B (Å^2)	0.63(3)	0.24(3)	0.20(3)	$=B_{O(31)}$
			n	0.5	0.5	0.5	
			R_p (%)	5.65	6.38	6.80	
			R_{wp} (%)	6.70	8.14	8.54	
			χ^2	1.609	2.400	2.447	

and calculated intensity profile of $Sr_3Ru_2O_7$ at 295 K, where we see that the fit of the model to the data is very good. The structural parameters and selected interatomic distances and angles obtained from the model are given in Tables II and III, respectively.

RESULTS AND DISCUSSION

Figure 4 shows the schematic representation of the structure of $Sr_3Ru_2O_7$. The unit cell contains four formula units. The two RuO_6 octahedra forming each bilayered block are rotated about the *c* axis with respect to one another by the same angle but in opposite directions. Since the octahedra share corners within each layer, these rotations cause a change of the *a* and *b* axes according to the axes transformation (1, −1, 0/1, 1, 0/0, 0, 1). The configuration of one block is, however, uncorrelated with that of the block in the next bilayer along the *c* axis, thus causing a splitting of the O(33) and O(34) sites. This feature can be described by saying that

TABLE III. Selected interatomic distances (Å), angles (°).

		295 K	25 K	9 K
Sr(11)-O(11)	×4	2.750 78(5)	2.738 50(5)	2.738 39(6)
Sr(11)-O(31)	×4	2.623(2)	2.611(2)	2.607(2)
Sr(11)-O(31)	×4	2.962(2)	2.990(2)	2.986(2)
Sr(12)-O(12)	×4	2.750 79(5)	2.738 50(5)	2.738 39(6)
Sr(12)-O(33)	×2	2.623(2)	2.611(2)	2.607(2)
Sr(12)-O(33)	×2	2.962(2)	2.990(2)	2.986(2)
Sr(12)-O(33)	×2	2.623(2)	2.611(2)	2.607(2)
Sr(12)-O(34)	×2	2.962(2)	2.990(2)	2.986(2)
Sr(21)-O(21)	×4	2.7567(2)	2.744 6(2)	2.744 4(2)
Sr(21)-O(22)	×1	2.459(2)	2.454(3)	2.452(3)
Sr(21)-O(31)	×2	2.524(2)	2.501(3)	2.506(2)
Sr(21)-O(31)	×2	2.865(2)	2.894(2)	2.896(2)
Sr(22)-O(22)	×1	2.7567(2)	2.744 6(2)	2.744 4(2)
Sr(22)-O(21)	×4	2.459(2)	2.454(3)	2.452(3)
Sr(22)-O(33)	×1	2.524(2)	2.501(3)	2.506(2)
Sr(22)-O(33)	×1	2.875(2)	2.894(2)	2.896(2)
Sr(22)-O(34)	×1	2.524(2)	2.501(3)	2.506(2)
Sr(22)-O(34)	×1	2.875(2)	2.894(2)	2.896(2)
Ru(1)-O(11)	×1	2.016(3)	2.022(2)	2.026(2)
Ru(1)-O(21)	×1	2.025(2)	2.042(3)	2.038(3)
Ru(1)-O(31)	×4	1.960 5(2)	1.955 7(2)	1.955 6(2)
Ru(2)-O(22)	×1	2.016(3)	2.022(2)	2.026(2)
Ru(2)-O(12)	×1	2.025(2)	2.042(3)	2.038(3)
Ru(2)-O(33)	×2	1.960 5(2)	1.955 7(2)	1.955 6(2)
Ru(2)-O(34)	×2	1.960 5(2)	1.955 7(2)	1.955 6(2)
Ru-O-Ru[a]		165.64(8)	163.90(8)	163.91(8)
Ru-O-Ru[b]		180	180	180

[a]In RuO_2 planes.
[b]Along *c* axis.

once the rotational configuration of a bilayer is chosen, the bilayer immediately above (or below) can be oriented, with equal probability, in two different ways; with the identical angular rotations in the same sense as the first bilayer, or with rotations by the same angle but in opposite directions. The uncorrelated nature of the blocks in the *c* direction creates a configuration in which the *c* parameter is defined only by the periodic shift of the (SrO)(SrO) bilayers and not by the orientation of the RuO_6 octahedra forming each block. For this reason, an equally valid description of the structure would be to fix both the occupancies of O(31) and O(32) at 0.5 and those of O(33) and O(34) at 1 (or 0) and 0 (or 1), respectively (see Fig. 4). The ordering of these atoms is therefore bidimensional, since their distribution has no periodicity along the *c* axis.

The structure of $Sr_3Ru_2O_7$ can also be described by the sequence of layers:

$$[(SrO)_o(RuO_2)_c(SrO)_o(RuO_2)_c(SrO)_o]$$
$$\times[(SrO)_c(RuO_2)_o(SrO)_c(RuO_2)_o(SrO)_c][(SrO)_o \ldots$$

where the square brackets include two corner-shared perovskite units. The subscripts *c* and *o* indicate if the cation is at the center or at the origin of the mesh for each layer. Ru atoms have octahedral coordinations. As we can see from Fig. 1, the Sr atoms, located between two RuO_2 layers within the block, have 12-fold coordination, while those located between two blocks, underlined in the sequence written above, are ninefold coordinated and the coordination polyhedron is a capped square antiprism. The structure is stacked along the *c* axis by blocks with the origin shifted by $a\sqrt{2}$ and $b\sqrt{2}$ from one to another and connected by Sr-O bonding. If the oxygen atoms on the RuO_2 planes were located at the ideal positions as reported in Ref. 13 (model I in Table I), the compound would be isostructural with $Sr_3Ti_2O_7$ (Ref. 19) with tetragonal symmetry $I4/mmm$. If the RuO_6 octahedra were rotated about the *c* axis with the rotations uncorrelated within the block of bilayers as well as between blocks, as it was found in the $Sr_3Ir_2O_7$ compound,[20] then the structure would retain the $I4/mmm$ symmetry (Table I, Model III), although this symmetry would be broken locally.

The correlated rotation of RuO_6 octahedra within the block of bilayers not only causes the oxygen atoms on the RuO_2 planes to shift away from the ideal positions and distorts the configuration of the $SrRuO_3$ perovskite, but it also changes the symmetry from tetragonal $I4/mmm$ to orthorhombic *Pban*, with parameters $a_{sup}=b_{sup}=a\sqrt{2}$, and $c_{sup}=c$. As mentioned before, with the exception of the oxygen atoms on the RuO_2 layers, all other atoms retain their $I4/mmm$ configuration. This may be explained by considering Fig. 5. The arrangement of the O atoms on the RuO_2 planes in block *A* has a fourfold rotation axis 4, while that in block *B* has an inversion axis 4. The combination reduces the symmetry to a twofold rotation axis, i.e., the overall symmetry changes from tetragonal to orthorhombic with lattice parameters $a=b\neq c$ and $\alpha=\beta=\gamma=90°$.

The ruthenium is coordinated by an elongated octahedron with 1.9605 Å for the four in-plane Ru-O distances, and 2.016 Å and 2.025 Å for the two apical distances. This octahedron is less distorted compared with that found in Sr_2RuO_4, where the Ru-O distances are 1.9364 Å for the

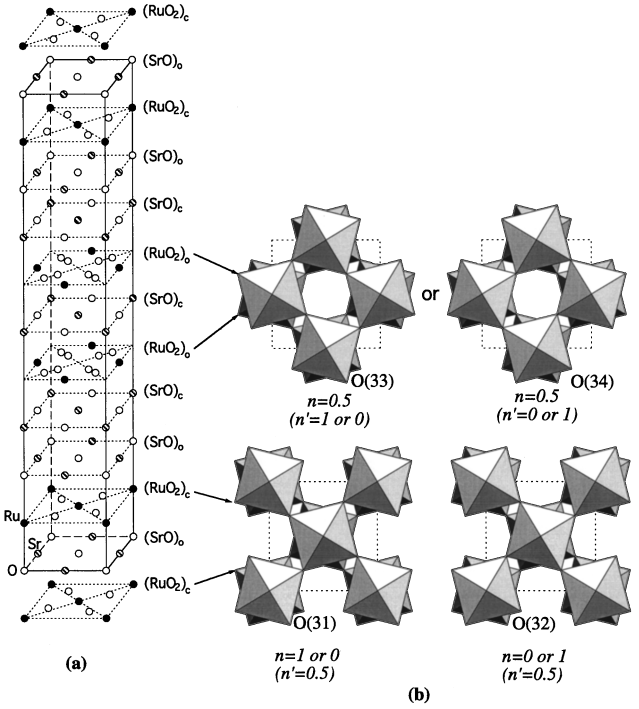

FIG. 4. (a) Schematic representation of the nuclear structure of the $Sr_3Ru_2O_7$, and of the sequence of layers. The symbols in each set of parentheses give the chemical composition of the layer, the subscripts *o* and *c* indicate if the cation is at the origin or in the center of the layer's mesh. (b) Projection of RuO_6 octahedra along the [001] direction, indicating the rotations of the octahedra. *n* and *n′* are site occupancies of the oxygen ions for two equivalent descriptions of the structure (see text).

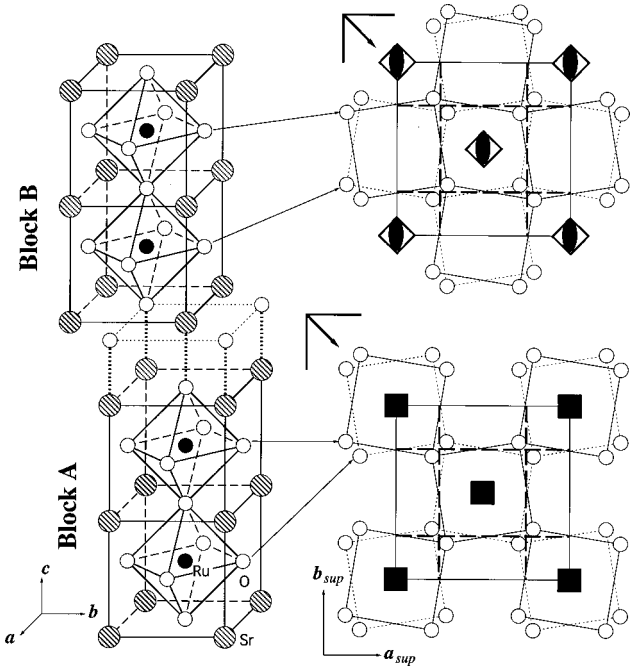

FIG. 5. Symmetry of two neighboring blocks in the structure of $Sr_3Ru_2O_7$, showing the generation of a twofold vertical symmetry axis. The symbols used for the symmetry elements are those used in the International Tables for Crystallography.

in-plane bonds and 2.067 Å for the apical bonds.[21] The rotation angles α of the RuO_6 octahedra are 7.18°, 8.05°, and 8.045° at 295, 25, and 9 K, respectively, thus showing a less pronounced distortion of the perovskite than that found in Sr_2IrO_4 (Ref. 21) and $Sr_3Ir_2O_7$,[20] where the corresponding rotations of the IrO_6 octahedra are ~11.4° and 11.8°, respectively. Due to the rotation of the octahedra around the *c* axis, the Ru-O-Ru in-plane bonding forms an angle of 165.6° at 295 K, while that along the *c* axis remains 180°. The 12-coordinated Sr has Sr to O distances ranging from 2.623 to 2.962 Å. The nine-coordinated Sr, on the other hand, is considerably displaced from the center of the antiprism toward the capped face, and the Sr-O bond distances range from 2.459 to 2.875 Å.

As the temperature decreases from 295 to 9 K, the lattice parameters *a* and *b* decrease from 5.5016 to 5.4769 Å as expected, while the *c* parameter increases from 20.7194 to 20.7963 Å. Thus there is a negative thermal expansion of the *c* axis in $Sr_3Ru_2O_7$. This expansion of the *c* axis is due to the behavior of the distortion of the RuO_6 octahedra as the temperature decreases. The average bond distance of Ru-O maintains a constant value of ~1.981 Å in the measured temperature range, while the Ru-O distance decreases for the bonds in the RuO_2 plane, and increases for the apical bonds. The increase of the apical distances is ~0.09 Å in total, and this is reflected in the increase of the *c* axis.

Finally, we discuss our attempts to observe magnetic order in this system. Diffraction measurements were performed in the temperature range from 1.4 to 250 K, using the BT-9 triple-axis spectrometer. Diffraction data were obtained for scattering angles in the range of 3°–65° at a series of temperatures to detect the development of new Bragg peaks, or to observe an increase in the nuclear Bragg peaks that might be associated with possible ferromagnetic ordering. No evidence was found for any long-range three-dimensional magnetic ordering, either ferromagnetic or antiferromagnetic, and any magnetic moment that might be ordering would have to be less than $\sim 0.05\mu_B$. This result contrasts with the reported ferromagnetic ordering at 104 K with an ordered Ru moment of $1.3\mu_B$, which we believe was due to a phase other than $Sr_3Ru_2O_7$.[17] We also carried out diffraction measurements with a 7-T magnetic field in the range above and below the broad maximum in the susceptibility at 15 K, but again observed no significant change in the intensities of any of the nuclear peaks. We also saw no statistically significant change in the diffuse scattering that might be associated with a spin-glass phase that is induced or modified by the field, and thus did not observe any scattering that is related to the weak maximum observed in the susceptibility. One possibility is that this susceptibility is associated with some kind of a frozen spin glass at low *T*, with a relatively small moment that is not particularly field sensitive. High-quality single-crystal samples that are free from intergrowth $SrRuO_3$ and Sr_2RuO_4 will likely be required to unravel the nature of the magnetism in this system.

ACKNOWLEDGMENT

We would like to thank A. Santoro for helpful discussions.

[1] J. J. Randall and R. Ward, J. Am. Ceram. Soc. **81**, 2629 (1959).
[2] A. Callaghan, C. W. Moeller, and R. Ward, Inorg. Chem. **5**, 1572 (1966).
[3] J. M. Longo, P. M. Raccah, and J. B. Goodenough, J. Appl. Phys. **39**, 1327 (1992).
[4] R. J. Bouchara and J. L. Gillson, Mater. Res. Bull. **7**, 873 (1972).
[5] F. Lichtenberg, A. Catana, J. Mannhart, and D. G. Schlom, Appl. Phys. Lett. **60**, 1138 (1992).
[6] C. B. Eom, R. J. Cava, R. M. Fleming, J. M. Phillips, R. B. van Dover, J. H. Marshall, J. W. P. Hsu, J. J. Krajewski, and W. F. Pack, Jr., Science **258**, 1766 (1992).
[7] C. B. Eom, R. B. van Dover, J. M. Phillips, J. D. Werder, J. H. Marshall, C. H. Chen, R. J. Cava, R. M. Fleming, and D. K. Fork, Appl. Phys. Lett. **63**, 2570 (1993).
[8] R. J. Cava, B. Batlogg, K. Kiyono, H. Takagi, J. J. Krajewski, W. F. Pack, Jr., L. W. Rupp, Jr., and C. H. Chen, Phys. Rev. B **49**, 890 (1994).
[9] Y. Maeno, H. Hashimoto, K. Yoshida, S. Nishizaki, T. Fijita, J. G. Bednorz, and F. Lichtenberg, Nature (London) **372**, 532 (1994).
[10] M. Braden, W. Reichardt, S. Nishizaki, Y. Mori, and Y. Maeno, Phys. Rev. B **57**, 1236 (1998).
[11] Y. Maeno, Physica C **282**, 206 (1997).
[12] J. A. Kafalas and J. M. Longo, J. Solid State Chem. **4**, 55 (1972).
[13] Hk. Müller-Buschbaum and J. Wilkens, Z. Anorg. Allg. Chem. **591**, 161 (1990).
[14] T. Williams, F. Lichtenberg, A. Reller, and G. Bednorz, Mater. Res. Bull. **26**, 763 (1991).
[15] S. Ikeda, Y. Maeno, and T. Fujita, Phys. Rev. B **57**, 978 (1998).
[16] R. J. Cava, H. w. Zandbergen, J. J. Krajewski, W. F. Peck, Jr., B. Batlogg, S. Carter, R. M. Fleming, O. Zhao, and L. W. Rupp, Jr., J. Solid State Chem. **116**, 141 (1995).
[17] G. Cao, S. McCall, and J. E. Crow, Phys. Rev. B **55**, R672 (1997).
[18] A. C. Larson and R. B. Von Dreele, Los Alamos National Laboratory Report No. LAUR086-748, 1990.
[19] S. N. Ruddlesden and P. Popper, Acta Crystallogr. **11**, 54 (1958).
[20] M. A. Subramanian, M. K. Crawford, and R. L. Harlow, Mater. Res. Bull. **29**, 645 (1994).
[21] Q. Huang, J. L. Soubeyroux, O. Chmaissem, I. Natali Sora, A. Santoro, R. J. Cava, J. J. Krajewski, and W. F. Peck, Jr., J. Solid State Chem. **112**, 355 (1994).